Draft version February 1, 2008
Preprint typeset using LaTeX style emulateapj v. 10/09/06

THE DENSITY PROFILE OF LOCAL ELLIPTICALS AS VIOLENTLY RELAXED, COLLISIONLESS, DISSIPATIONLESS SYSTEMS

Eduard Salvador-Solé[1]*, Sinue Serra[1], Rosa Domínguez-Tenreiro[2], and Alberto Manrique[1]

Draft version February 1, 2008

ABSTRACT

In a series of recent papers, a new formalism has been developed that explains the inner structure of dark matter halos as collisionless, dissipationless systems assembled through mergers and accretion at the typical cosmological rate. Nearby ellipticals are also collisionless, dissipationless systems assembling their mass through mergers, but contrarily to the former structures they do not continuously accrete external matter because they are shielded by their host halos. Here we explore the idea that the infall of their own matter ejected within the halo on the occasion of a violent merger can play a role similar to external accretion in halos. The predicted stellar mass density profile fits the observed one, and the empirical total mass density profile is also recovered.

Subject headings: gravitation — galaxies: formation — galaxies: structure — galaxies: elliptical and lenticular — galaxies: halos — dark matter

1. INTRODUCTION

Nowadays there is increasing evidence about the important role of major, non-dissipative mergers (Toomre & Toomre 1972) in the mass assembly of elliptical galaxies (Conselice 2003; Bell et al. 2005) at intermediate or low-redshifts, the formation of their stellar populations and the dissipative processes previous to it having occured mainly at high-z (Faber et al. 2005; de Lucia et al. 2005; Domínguez-Tenreiro et al. 2006). The problem with dissipationless major mergers is that there is no known analytical treatment for the violent relaxation (Lynden-Bell 1967) they lead to.

Elliptical galaxies are similar to cold dark matter (CDM) halos in many respects. Apart from the similar role played by major, non-dissipative mergers in their mass assembly, their mass, velocity dispersion, and length scales show systematic regularities and correlations that can be related with each other (Bernardi et al. 2003; Graham et al. 2006; Oñorbe et al. 2007). Likewise, their 3D density profiles are all well fit (Navarro et al. 2004; Merritt et al. 2005; Merritt et al. 2006; Oñorbe et al. 2007) by the Einasto (Einasto & Haud 1969) law or the Prugniel-Simien (1997) approximate analytical inversion of the projected Sérsic (1968) law. These coincidences suggests that these profiles could have been shaped by similar physical processes.

In a series of recent papers, a new formalism has been developed (Salvador-Solé et al. 2007, hereafter SMGH and references therein) that explains the inner structure of halos from the very collisionless, dissipationless nature of CDM, and which predicts halo structural and kinematic properties that are in good agreement with the results of N-body simulations (González-Casado et al. 2007). Thus, it is natural to consider whether this formalism can also explain the inner structure of ellipticals.

*[1]Departament d'Astronomia i Meteorologia, Institut de Ciències del Cosmos (UB-IEEC), associated with the Consejo Superior de Investigaciones Científicas, Universitat de Barcelona, Spain; [2] Departamento de Física Teórica, C-XI. Universidad Autónoma de Madrid, Spain

But things are not that simple. Halos are permanently accreting external matter, while ellipticals are not. As numerical simulations show (e.g., Domínguez-Tenreiro et al. in preparation), matter falling into the halo is too energetic to stick to the center, and it is deposited at the edge of the system. Only clumps massive enough are braked by dynamical friction and spiral down until merging with the central galaxy. Therefore, apart from such discrete (minor and major) mergers there is no continuous accretion into central ellipticals.

This is a crucial difference in the context of the SMGH model because in that model the structure of halos is determined precisely by their continuous accretion. Indeed, the profile at the edge of a halo of any extensive property is set by the rates of infalling and rebounding matter, which do not depend on the particular inner mass distribution but only on the current accretion rate. As CDM is collisionless, the spatial distribution of any property is necessarily at all derivative orders, implying that the whole respective inner profile adapts to the external one defined by accretion. As CDM is in addition dissipationless, the steady inner region remains unaltered during accretion, causing the profiles to grow from the inside out. This specific growth allows us to infer the profile of any extensive property from its typical rate of increase by accretion (see below for the case of the density profile).

Although local ellipticals do not accrete external matter, for a short interval after a merger they do collect the (bound) matter ejected in that violent event. The aim of the present Letter is to explore the possibility that such an infall of ejecta can play a similar role in ellipticals as that plaied by cosmological accretion in dark halos.

2. DYNAMICS OF EJECTA

When two galaxies pass each other close enough to be tidally disrupted their content is ejected in all directions. As the disruption takes place when the merging galaxies are orbiting around the center of mass, the typical radius $R_{\rm p}$ of the ejection region is larger than the half-mass radii $r_{\rm e}$ of the progenitors. The particle velocities in the disrupted system should be approximately normally

distributed,

$$f(\mathbf{v}) \propto \exp\left[-\frac{3v^2}{2\sigma_{\rm p}^2}\right], \quad (1)$$

with both the proportionality factor and the characteristic 3D velocity dispersion $\sigma_{\rm p}$ independent of the particle mass (the acceleration undergone by particles does not depend on it).

Particles ejected at larger radial velocities expand more rapidly than those ejected at smaller ones. Furthermore, for a given velocity, particles ejected from inner regions experience a smaller gravitational pull and expand more rapidly than those ejected from outer regions. Therefore, ejecta tend to segregate into concentric shells with outwards increasing radial velocities. Most of these shells follow bound orbits. They reach the apocenter and fall back, cross the central region and rebound to a somewhat smaller turn-around radius owing to the crossing with shells falling in for the first time, and so forth. The result of this chaotic motion is a central relaxed object into which bound ejecta continue to fall and rebound for some time.

These dynamics greatly resemble those of the cosmological evolution of density perturbations, with the difference that in the present case, apart from the shell-crossing between infalling and rebounding layers, there is some additional shell-crossing owing to the finite size of the ejection region as there tends to be segregation of particles according to radial velocities. In the present Letter, we do not consider these finite size effects. We focus on the density profile of the steady object that would emerge were all particles ejected from the same typical radius $R_{\rm p}$, and the above mentioned segregation would be instantaneously and perfectly achieved. In these circumstances, some known results for the collapse of spherical density perturbations hold.

If rebounding shells were suppressed, there would be no shell-crossing (see below) and the stellar mass $M(v)$ inside the shell with positive initial radial velocity v would be constant and equal to the total mass of shells with smaller velocities. Taking into account equation (1), after integrating over the tangential velocity components, we obtain for a radial velocity v

$$M(v) = A\int_0^v {\rm d}\tilde{v}\, \exp\left(-\frac{3\tilde{v}^2}{2\sigma_{\rm p}^2}\right) = \sqrt{\frac{\pi}{6}} A\sigma_{\rm p}\, {\rm erf}\left(\frac{\sqrt{3}v}{\sqrt{2}\sigma_{\rm p}}\right). \quad (2)$$

Similarly, the constant energy of stars inside that shell (for the system truncated at its radius and the potential origin at infinity) is

$$E(v) = A\int_0^v {\rm d}\tilde{v}\left[\frac{\tilde{v}^2}{2} + \frac{\sigma_{\rm p}^2}{3} - \frac{GM(\tilde{v})}{\eta R_{\rm p}} + \Phi_{\rm h}(R_{\rm p})\right] \times \exp\left(-\frac{3\tilde{v}^2}{2\sigma_{\rm p}^2}\right). \quad (3)$$

The integrals in equations (2) and (3) extend over *positive* radial velocities only because particles with negative initial radial velocity, $-v$, cross the system, and join the shell with v, the time required to do so being one of the finite size effects we ignore. By taking v equal to infinity in these equations, we arrive at

$$\sigma_{\rm p}^2 = \frac{2E_{\rm p}}{M_{\rm p}} + \frac{GM_{\rm p}}{\eta R_{\rm p}} - 2\Phi_{\rm h}(R_{\rm p}) \quad \text{and} \quad A = \sqrt{\frac{6}{\pi}}\frac{M_{\rm p}}{\sigma_{\rm p}}, \quad (4)$$

relating the velocity dispersion $\sigma_{\rm p}$ and the normalization constant A, which is equal to the proportionality factor in equation (1) times the average particle mass[1], to the typical ejection radius $R_{\rm p}$ and the total stellar mass $M_{\rm p}$, energy $E_{\rm p}$, and baryon mass fraction η of ejecta. In equations (2) and (3), G is the gravitational constant and

$$\Phi_{\rm h}(r) = -4\pi G\rho_0\, r_{\rm h}^2\, n_{\rm h} P\left[3n_{\rm h}, (r/r_{\rm h})^{1/n_{\rm h}}\right] \times \left(\frac{r_{\rm h}}{r}\Gamma(3n_{\rm h}) + \Gamma(2n_{\rm h})\left\{1 - P\left[2n_{\rm h}, (r/r_{\rm h})^{1/n_{\rm h}}\right]\right\}\right) \quad (5)$$

is the potential of the steady dark halo, endowed with an Einasto density profile (SMGH),

$$\rho(r) = \rho_0\, \exp\left[-\left(\frac{r}{r_{\rm h}}\right)^{1/n_{\rm h}}\right], \quad (6)$$

with two independent shape parameters, say, $n_{\rm h}$ and $r_{\rm h}$ for one fixed total mass $M_{\rm h}$. In equation (5), $\Gamma(x)$ is the gamma function and $P(a,x)$ is defined as

$$P(a,x) = \frac{1}{\Gamma(a)}\int_0^x {\rm d}\xi\, \exp(-\xi)\, \xi^{a-1}. \quad (7)$$

In deriving equation (3), we have taken into account that, as the CDM distribution in the steady halo adapts to external accretion, the void left by the ejected dark matter will be rapidly filled again, causing the net amount of ejected CDM to decrease. For this reason, η may be substantially larger than the original baryon mass fraction $\eta_{\rm p}$ within $R_{\rm p}$, the relation between the values being

$$\eta = \frac{M_{\rm p}}{\eta_{\rm p}^{-1}M_{\rm p} - M_{\rm h}(R_{\rm p})}, \quad (8)$$

where $M_{\rm p}$ is the total ejected stellar mass and

$$M_{\rm h}(r) = 4\pi\rho_0 r_{\rm h}^3 n_{\rm h}\, \Gamma(3n_{\rm h}) P\left[3n_{\rm h}, (r/r_{\rm h})^{1/n_{\rm h}}\right] \quad (9)$$

is the steady halo mass inside r for the Einasto density profile (eq. [6]).

As mentioned above, rebounding and shell-crossing lead to a steady state object, which extends, at any given time t, out to the limiting radius $R(t)$. This radius can be estimated from the virial relation $W(t) = 2E(t)$, where $W(t)$ is the potential energy of the relaxed stellar system, truncated at $R(t)$ and assumed to have a uniform mass distribution, and $E(t)$ the corresponding conserved (in the previous model with no shell-crossing) total energy. Estimating $E(t)$ is at turn-around and assuming a uniform mass distribution, in the absence of any external gravitational potential, leads to $R(t)$ equal to half the turn-around radius (Gunn & Gott 1972). In the present case, $E(t)$ is given directly by equation (3) where v is equal to the initial radial velocity of the shell collapsing at t. Dividing that virial relation by the corresponding inner stellar mass (eq. [2]), we are led to the following implicit equation for $R(v)$

$$-\frac{GM(v)}{\eta R(v)} + \Phi_{\rm h}[R(v)] = v^2 + \frac{2\sigma_{\rm p}^2}{3} - \frac{2GM(v)}{\eta R_{\rm p}} + 2\Phi_{\rm h}(R_{\rm p}). \quad (10)$$

[1] The particle mass factorizes because the velocity distribution function (1) does not depend on it.

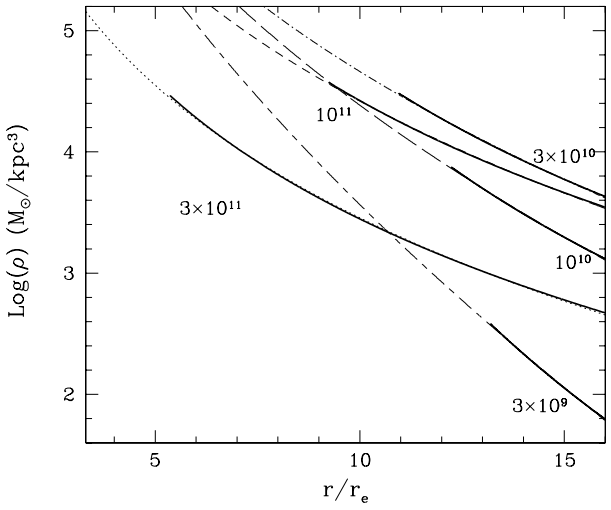

FIG. 1.— Typical Prugniel-Simien density profiles for ellipticals with stellar masses equal to 3×10^9 $M_\odot$ (long-short-dashed line), 10^{10} $M_\odot$ (dot-dashed line), 3×10^{11} $M_\odot$ (dashed line), and $\times 10^{11}$ $M_\odot$ (dotted line) according to Graham et al. (2006 and references therein) and their best fit by the theoretical density profile derived here (solid lines). See Table 1 for the values of the respective parameters.

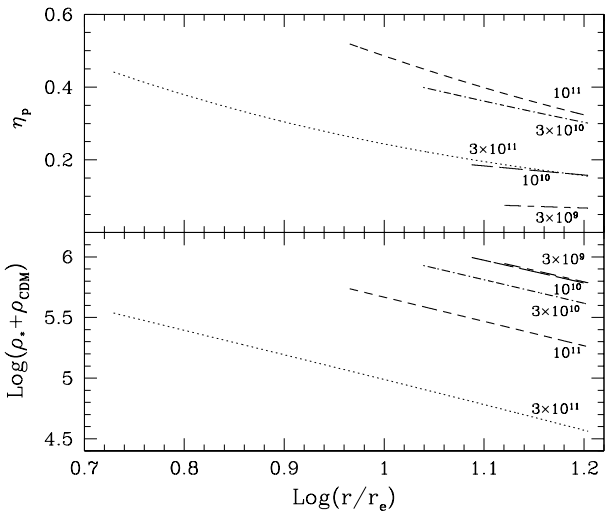

FIG. 2.— Baryon mass fraction (top panel) and total (baryon or stellar plus CDM) density profiles (bottom panel) for the theoretical ellipticals (same symbols) plotted in Figure 1.

The initial velocity v of the shell collapsing at t is simply the inverse of the collapse time, in the model with no shell-crossing, of the shell that starts with v. This collapse time, $t_{\rm coll}(v)$, can be obtained by numerical integration of the equation of motion

$$\ddot{r} = -\frac{G\left\{\eta^{-1}M(v) + M_{\rm h}[r(t)]\right\}}{r^2}\,, \qquad (11)$$

then imposing $r(t)$ equal to zero. We have checked that $t_{\rm coll}(v)$ is an increasing function of v, which proves that there would be no shell-crossing if the rebounding shells were suppressed.

The density profile of the steady object at t can be obtained in the way explained in SMGH provided the structure is stable against the infall of ejecta which warrants its inside-out growth. In other words, the characteristic time of stellar mass collapse (in the model with no shell-crossing), inverse of the collapse rate $\mathcal{R}_{\rm a} \equiv \dot{M}/M$, must be larger than the crossing time for particles at $R(t)$ for every collapse time t or, equivalently, for every initial velocity v of bound shells,

$$\mathcal{R}_{\rm a}^{-1}(v) > \left[\frac{\eta R^3(v)}{2GM(v)}\right]^{1/2} \qquad (12)$$

where

$$\mathcal{R}_{\rm a}(v) = \frac{1}{M(v)}\frac{{\rm d}M(v)}{{\rm d}v}\left(\frac{{\rm d}t_{\rm coll}}{{\rm d}v}\right)^{-1}\,. \qquad (13)$$

Condition (12) is satisfied, so the SMGH model holds.

3. PREDICTED DENSITY PROFILE

Given the inside-out growth of the steady system, its mass evolves according to the equation

$$M(t) = \int_0^{R(t)} {\rm d}r\, 4\pi\rho(r)\, r^2\,, \qquad (14)$$

where the density ρ is independent of time. Differentiating equation (14) leads to the density profile $\rho[R(t)]$ in terms of the time derivatives of both the collapsing mass $M(t)$ and the virial radius $R(t)$. More simply, by expressing $M(t)$ and $R(t)$ as $M[v(t)]$ and $R[v(t)]$ and differentiating equation (14) by means of the chain rule, the time derivative of v simplifies out, and, after some algebra, we are led to the following parametric equations for the density profile we want,

$$\rho(v) = \frac{M(v) + \eta M_{\rm h}[R(v)]}{4\pi R^3(v)} \times\left\{1 - \frac{2R(v)}{R_{\rm p}}\left[1 - \sqrt{\frac{\pi}{6}}\frac{\eta R_{\rm p}\sigma_{\rm p} v}{GM_{\rm p}}\exp\left(\frac{3v^2}{2\sigma_{\rm p}^2}\right)\right]\right\}^{-1} \qquad (15)$$

and $R(v)$ given by equation (10).

In Figure 1, we plot the typical 3D density profiles of the Prugniel-Simien form,

$$\rho(r) = \rho_{\rm e}\left(\frac{r}{r_{\rm e}}\right)^{-p}\exp\left\{-d_n\left[\left(\frac{r}{r_{\rm e}}\right)^{1/n} - 1\right]\right\}, \qquad (16)$$

for present day ellipticals of various stellar masses M. For $\rho_{\rm e}$ equal to the density at the half-mass radius $r_{\rm e}$, d_n and p become functions of n, approximately given, for $n \gtrsim 0.5$, by $2n - 1/3 + 0.009876/n$ and $1.0 - 06097/n + 0.05463/n^2$, respectively (see Merrit et al. 2006). Thus, the profile (16) is fixed by three independent parameters, reducing to two for one given mass M. The typical values of these parameters have been taken from Graham et al. (2006 and references therein); see Table 1.

Galaxy	Observed Profile			CDM Halo				Predicted Profile		
$M/10^{10}$ ($M_\odot$)	n	$r_{\rm e}$ (kpc)	$\log \rho_{\rm e}$ ($M_\odot$ pc^{-3})	$M_{\rm h}/10^{12}$ ($M_\odot$)	$n_{\rm h}$	$r_{\rm h}/10^8$ (kpc)	$\log \rho_0$ $M_\odot$ pc^{-3})	$R_{\rm p}$ (kpc)	$\sigma_{\rm p}$ (km s^{-1})	$\eta_{\rm p}$
0.3	1.70	0.94	−0.94	0.20 (0.05)	6.7 (6.2)	0.47 (0.09)	2.4 (2.2)	24.9 (21.7)	60.0 (36.0)	0.05 (0.16)
1.0	2.34	1.12	−0.70	0.35 (0.13)	7.0 (6.6)	0.25 (0.71)	2.5 (2.3)	27.4 (18.6)	92.0 (76.0)	0.14 (0.27)
3.0	3.10	1.57	−0.72	0.55 (0.42)	7.2 (7.1)	0.15 (0.20)	2.6 (2.5)	34.3 (34.7)	126 (112)	0.23 (0.28)
10	4.28	3.16	−1.17	1.40 (1.40)	7.7 (7.7)	3.85 (3.85)	2.9 (2.9)	58.4 (58.4)	197 (197)	0.29 (0.29)
30	5.72	10.0	−2.26	4.50 (4.25)	8.4 (8.4)	49.6 (55.4)	3.3 (3.3)	99.7 (108)	355 (335)	0.27 (0.28)

TABLE 1

For each empirical profile, we also plot in Figure 1 its best fit to the theoretical profile given by equations (15) and (10). As ejecta are rapidly collected by the newborn elliptical (most bound mass is collected in less than one Gyr), its typical stellar mass M has been assumed to coincide with the final asymptotic value,

$$M = M_{\rm p} - A\int_{v_{\rm esc}}^{\infty} {\rm d}\tilde{v}\exp\left(-\frac{3\tilde{v}^2}{2\sigma_{\rm p}^2}\right) = M_{\rm p}\,{\rm erf}\left[\frac{\sqrt{3}}{\sigma_{\rm p}}\left(\frac{GM_{\rm p}}{\eta R_{\rm p}} - \Phi_{\rm h}(R_{\rm p})\right)^{1/2}\right] \qquad (17)$$

where $v_{\rm esc} = \sqrt{2GM_{\rm p}/(\eta R_{\rm p}) - 2\Phi_{\rm h}(R_{\rm p})}$ is the escape velocity at $R_{\rm p}$. Then, the typical total dark halo mass $M_{\rm h}$ has been obtained from M by means of the relation by Shanks et al. (2006). According to these authors, the ratio of dark halo to stellar mass, equal to ~ 14 for normal ellipticals (see also Oñorbe et al. 2007), rapidly increases towards the dwarf mass end. But the estimate is quite uncertain there. For this reason, we have also considered the assumption of an ever constant dark halo to stellar mass ratio equal to 14. Then, the Einasto shape parameters fixing the CDM halo density profile have been obtained using the SMGH prescription ignoring any adiabatic contraction. Having fixed all these values (see Table 1) there are only three free parameters to be adjusted: $\sigma_{\rm p}$, $R_{\rm p}$, and $\eta_{\rm p}$.

As can be seen from Figure 1, the theoretical profile yields a very good fit for very reasonable values of those free parameters (see Table 1): $\sigma_{\rm p}$ takes values of the order of (or slightly larger than) the typical velocity dispersion of the progenitors, $R_{\rm p}$ takes values of the order of their limiting radii, and $\eta_{\rm p}$ of the order of their total baryon mass fraction, (see Fig. 13 in Oñorbe et al. 2007).

Figure 2 shows the predicted baryon mass fraction and total (stellar plus CDM) density profiles, which also agree very well with empirical data (Koopmans et al. 2006; Oñorbe et al. 2007). Note, in particular, the isothermal-like behavior of the total density profiles.

4. CONCLUSIONS

These results seem to confirm that the structure of nearby ellipticals (and of simulated non-accreting CDM halos; see Hansen et al. 2005) is set in major mergers (minor mergers let it essentially unaltered), in the way explained in SMGH through the infall of matter ejected at that violent event. At this stage, we found no evidence of a different formation mechanism for dwarf ellipticals compared to normal bright ones.

In the present Letter, all ejecta were assumed to be thrown from the same typical radius. This limits severely the minimum radius down to which the predicted density profile can be calculated to only $\sim R_{\rm p}/2$ (exactly the value in the absence of a dark halo; see eq. [10]), corresponding to the virial radius for shells initially at rest (at turn-around). In a forthcoming paper, we will apply a more accurate treatment that will allow us to reach the galaxy center. In that paper, we will aso deal with the kinematics of ellipticals.

This work was supported by the Spanish DGES grant AYA2006-15492 and by the regional government of Madrid through the ASTROCAM Astrophysics network (S-0505/ESP-0237). SS benefited from a grant from the Institut d'Estudis Espacials de Catalunya.

REFERENCES

Bernardi M., et al. 2003, AJ, 125, 1866
Bell, E.F., et al. 2005, astro-ph/0506425 preprint
Conselice, C.J. 2003, ApJS, 147, 1
de Lucia, G., Springel, V., White, S.D.M., Croton, D., & Kauffmann, G. 2005, astro-ph/0509725 preprint
Domínguez-Tenreiro R., Oñorbe J., Sáiz A., Artal H., & Serna A., 2006, ApJ, 636, L77
Einasto, J., & Haud U., 1989, A&A 223, 89
Faber, S.M., et al. 2005, astro-ph/0506044 preprint
Graham, A. W., Merritt, D., Moore, B., Diemand J., & Tersić, B., 2006, ApJ, 132, 2711
González-Casado, G., Salvador-Solé, E., Manrique, A., & Hansen, S. H. 2007 Submitted to ApJ, [arXiv: astro-ph/072368]
Gunn J. E., & Gott J. R., 1972, ApJ, 176, 1
Hansen, S. H., Moore, B., Zemp, M., & Stadel, J. 2006, JCAP, 1, 14
Koopmans, L. V. E., et al. 2006, ApJ, 649, 599
Lynden-Bell D., 1967, MNRAS, 136, 101
Merritt, D., Navarro J. F., Ludlow, A., & Jenkins A. 2005, ApJ 624, L85 ApJ, 132, 2685
Merritt, D., Graham, A. W., Moore, B., Diemand J., & Tersić, B. 2006, ApJ, 132, 2685
Navarro, J. F., et al. 2004, MNRAS 349, 1039
Oñorbe, J., Domínguez-Tenreiro, R., Sáiz, A., & Serna, A. 2007, to be published in MNRAS [arXiv: astro-ph/0612732]
Prugniel, P., & Simien, F. 1997, A&A 321, 111
Salvador-Solé, E., Manrique, A. González-Casado, G., & Hansen, S. H. 2007 Submitted to ApJ, [arXiv: astro-ph/071134] (SMGH)
Shankar, F., Lapi, A., Salucci, P., De Zotti, G., Danese, L. 2006, ApJ, 643, 14S
Sérsic, J.-L. 1968, Atlas de Galaxias Australes (Córdoba: Univ. Córdoba)
Toomre, A., & Toomre J. 1972, ApJ, 178, 623